Tetrahedron 68 (2012) 9936–9941

Contents lists available at SciVerse ScienceDirect

Tetrahedron

journal homepage: www.elsevier.com/locate/tet

Fluorescence properties of indolenine semi-squarylium dyes

Masaki Matsui *, Toshihiro Shibata, Masato Fukushima, Yasuhiro Kubota, Kazumasa Funabiki

Department of Materials Science and Technology, Faculty of Engineering, Gifu University, 1-1 Yanagido, Gifu 501-1193, Japan

ARTICLE INFO

Article history:
Received 27 August 2012
Received in revised form 18 September 2012
Accepted 20 September 2012
Available online 26 September 2012

Keywords:
Fluorescence
Indolenine semi-squarylium dye
Solid-state fluorescence
Single X-ray crystallography
Aggregation-induced emission enhancement

ABSTRACT

3-Butoxy-4-(1-butyl-3,3-dimethyl-3*H*-indol-2-ylidenemethyl)-3-cyclobut-1,2-dione exhibited the most intense florescence at fluorescence maxima 536 and 563 nm with fluorescence quantum yield 0.21 among any indolenine semi-squarylium dyes in the crystalline form due to the isolated dimer-type molecular packing and its suitable melting point. This compound showed aggregation-induced emission enhancement.

© 2012 Elsevier Ltd. All rights reserved.

1. Introduction

Survey of solid-state fluorescent organic compounds is one of the most exciting subjects in connection with development of emitters in OLED,[1] solid dye laser,[2] and probes.[3] Though many compounds show fluorescence in solution, less compounds exhibit fluorescence in the solid state. Semi-squarylium (semi-SQ) dyes are known as the intermediates for the preparation of unsymmetrical SQ,[4] cationic SQ,[5] and bisSQ dyes.[6] The potential applications of semi-SQ dyes for sensors[7] and sensitizers[8] have been also reported. On the other hand, recently, survey of new materials, such as siloles,[9] tetraarylethylenes,[10] and triarylethylenes[11] showing aggregation-induced emission enhancement (AIEE) has been attracted large attention. AIEE has been usually reported to come from the inhibition of free rotation of C–Ar bonds in the aggregated form. We consider that other flexible linkage, such as C–O bonds can also cause AIEE. We report herein the fluorescence properties of indolenine semi-SQ dyes.

2. Results and discussion

2.1. Synthesis

Indolenine semi-SQ dyes **11**–**16** were synthesized as shown in Scheme 1. 2,3,3-Trimethylindolenine (**1**) was allowed to react with alkyl iodides **2**–**4** to give *N*-alkylindolenium iodides **5**–**7**, followed by the reaction with dialkyl squarates **8**–**10** to afford **11**–**15**. Semi-SQ dye **13** was hydrolyzed to give **16**. Semi-SQ dyes **11**, **13**, and **16** are known compounds.

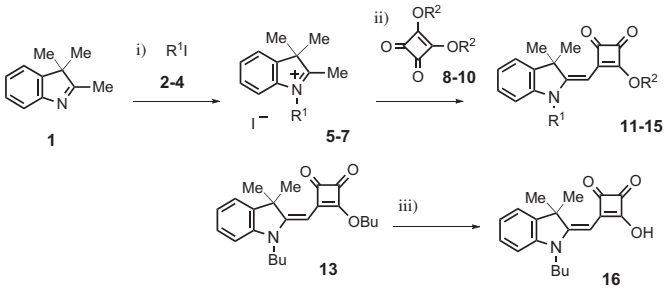

Compd	R^1
2, 5	Me
3, 6	Bu
4, 7	Oct

Compd	R^2
8	Me
9	Bu
10	Oct

Compd	R^1	R^2
11	Me	Bu
12	Bu	Et
13	Bu	Bu
14	Bu	Oct
15	Oct	Bu

Scheme 1. Reagents and conditions: i) **1** (1.0 equiv), **2**–**4** (3.3 equiv), reflux, MeCN, 1 day, ii) **5**–**7** (1.0 equiv), **8**–**10** (1.0 equiv), TEA, alcohol, 75 °C, 0.3–2 h, iii) **13** (1.0 equiv), aq NaOH, reflux, 5 min, then 2 N HCl.

2.2. UV–vis absorption and fluorescence spectra

The UV–vis absorption and fluorescence spectra of **13** in various solvents are shown in Fig S7. Compound **13** showed the most intense fluorescence in ethanol. Fig. 1 depicts the UV–vis absorption

* Corresponding author. Tel.: +81 58 293 2601; fax: +81 58 293 2794; e-mail address: matsuim@gifu-u.ac.jp (M. Matsui).

0040-4020/$ – see front matter © 2012 Elsevier Ltd. All rights reserved.
http://dx.doi.org/10.1016/j.tet.2012.09.089

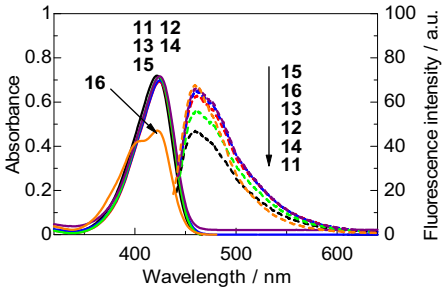

Fig. 1. UV–vis absorption spectra of **11**–**16** in ethanol. Measured on 1×10^{-5} mol dm^{-3} of substrate at 25 °C. Solid and dotted lines represent UV–vis absorption and fluorescence spectra, respectively.

and fluorescence spectra of **11**–**16** in ethanol. The results are also summarized in Table 1. The absorption maximum (λ_{max}) was observed at around 425 nm. The molar absorption coefficient (ε) was calculated to be ca. 70,000 dm^3 mol^{-1} cm^{-1} except for **16** (44,100). The fluorescence maximum (F_{max}) was observed at around 460 nm. The Stokes shift was small, there being ca. 36 nm. They showed similar fluorescence spectra with low fluorescence quantum yield (Φ_f, <0.01). Thus, no remarkable differences in the UV–vis absorption and fluorescence spectra were observed among **11**–**16** in ethanol.

Table 1
UV–vis absorption and fluorescence spectra of **11**–**16**

Compd	In ethanol[a]				Solid state		
	λ_{max} (ε_{max}) nm	F_{max} nm	Φ_f[b]	SS[c] nm	λ_{ex}[d] nm	F_{max} nm	Φ_f[b]
11	422 (71,900)	460	<0.01	38	427	511, 546	<0.01
12	424 (71,400)	461	<0.01	36	425	526, 545	<0.01
13	425 (69,200)	461	<0.01	36	435	536, 563	0.21
14	424 (69,700)	460	<0.01	36	425	502	<0.01
15	425 (69,800)	461	<0.01	35	425	522	0.02
16	423 (44,100)	459	<0.01	36	425	—[e]	—[e]

[a] Measured at the concentration of 1×10^{-5} mol dm^{-3} at 25 °C.
[b] Determined by absolute PL quantum yield measurement system C9920-02.
[c] Stokes shift.
[d] Excitation wavelength determined by diffuse reflection spectra given by Kubelka–Munk units.
[e] Too weak.

2.3. AIEE test

The AIEE test was performed for **13** and **16**. The results are shown in Figs. 2 and 3. In the case of **13**, the test was performed in ethanol–water mixed solvent. Weak fluorescence peak was

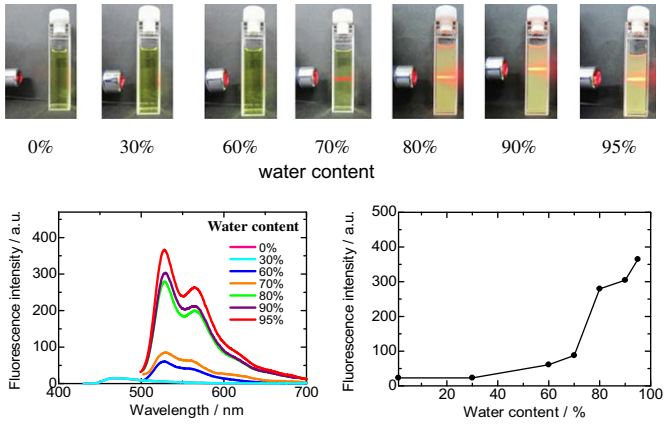

Fig. 2. AIEE test for **13**. Measured on 1×10^{-4} mol dm^{-3} of **13** in ethanol–water mixed solvent at 25 °C.

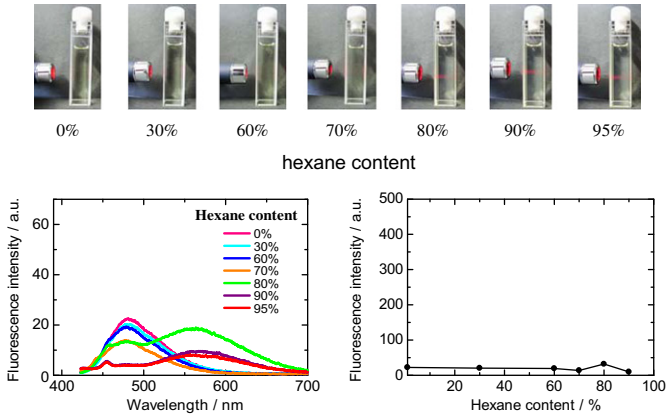

Fig. 3. AIEE test for **16**. Measured on 1×10^{-5} mol dm^{-3} of **16** in ethyl acetate–hexane mixed solvent at 25 °C.

observed at around 460 nm in 0 and 30% water content. The mixed solvent was almost transparent when the water content is less than 60%. In 70% water content, apparent Tyndall scattering was observed. Then, as higher was the water content, the solvent became opaque. At the same time, the fluorescence peaks at around 535 and 560 nm comes from the aggregated form drastically increased. The intensity is much stronger than that in 0% water content. Thus, semi-SQ dye **13** showed clear AIEE.

As semi-SQ dye **16** is soluble in water, the AIEE test was performed in ethyl acetate–hexane mixed solvent. In 0, 30, and 60% hexane content, weak fluorescence peak was observed at 480 nm. This peak gradually decreased with increasing hexane content. Tyndall scattering was observed in 80% hexane content and new emission from the aggregated form was observed at around 560 nm. Then, this emission decreased by adding hexane. Thus, though semi-SQ dye **16** showed very weak fluorescence in the aggregated form, no clear AIEE was observed.

To understand why dye **13** shows AIEE, the effects of solvent and temperature on the UV–vis absorption and fluorescence spectra of **13** and **16** were examined. The results are indicated in Figs. 4 and 5. Fig. 4(a) depicts that though no significant differences in the UV–vis absorption spectra of **13** are observed in diethylene glycol (DEG, velocity (η): 30 cp at 25 °C) and in ethanol (η: 1.06 cp at 25 °C), the fluorescence intensity of **13** in DEG is 4.8-times stronger

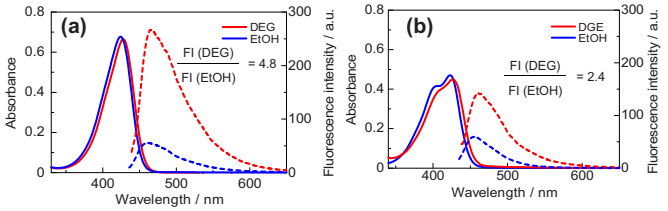

Fig. 4. UV–vis absorption and fluorescence spectra of (a) **13** and (b) **16** in diethylene glycol (DEG) and ethanol at 25 °C. Measured on 1×10^{-5} mol dm^{-3} of substrate.

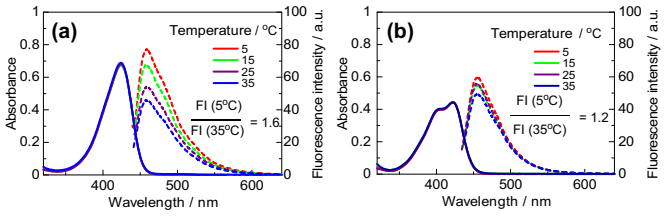

Fig. 5. UV–vis absorption and fluorescence spectra of (a) **13** and (b) **16** at 5, 15, 25, and 35 °C in ethanol. Measured on 1×10^{-5} mol dm^{-3} of substrate.

than that in ethanol. Meanwhile, in the case **16**, only 2.4-times as shown in Fig. 4(b).

Fig. 5(a) shows that though the UV–vis absorption spectra of **13** at 5 and 35 °C are identical, the fluorescence of **13** at 5 °C is 1.6-times more intense than that at 35 °C. Fig. 5(b) indicates that the fluorescence intensity of **16** at 5 °C is only 1.2-times stronger than that at 35 °C. These results suggest that the free rotation of flexible C–O bonds of **13** were inhibited in the aggregated form to exhibit AIEE.

2.4. Solid-state fluorescence

The solid-state fluorescence spectra of **11**–**16** recrystallized from hexane are shown in Fig. 6. No clear fluorescence spectrum was observed for **16**. Compounds **11**, **12**, **14**, and **15** showed weak fluorescence. Interestingly, semi-SQ dye **13** significantly exhibited intense florescence. The Φ_f 0.21 is remarkably greater than that in solution (<0.01). The F_{max} at 536 and 563 nm could come from S_1 to S_0 transition and the vibration level, respectively. The F_{max} are more bathochromic compared with that in ethanol (461 nm), showing intermolecular interactions in the solid state.

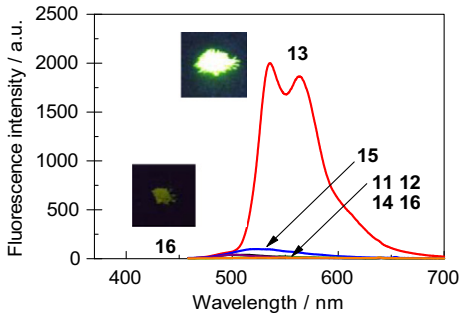

Fig. 6. Solid-state fluorescence spectra of **11**–**16**.

2.5. Single X-ray crystallography

To understand why **13** exhibited intense fluorescence in the crystalline form, the single X-ray crystallographic analysis of **11**, **12**, **13**, **14**, and **15** was performed.

The single X-ray crystallography of **11** is shown in Fig. 7. Side view (1) depicts that molecules are arranged as a 'bricks-in-a-wall' fashion. Side view (1), (2) and top view (1), (2) indicate that molecules A, B, and C are located on the same plane and are aligned toward the same direction. CH/O interactions are observed among A, B, and C. π/π-interactions are observed between B and D at the squarate moiety, there being the interplanar distance 3.51 Å. The same interactions are observed between B and G. Thus, dye **11** has consecutive π/π stacking as shown in side view (1).

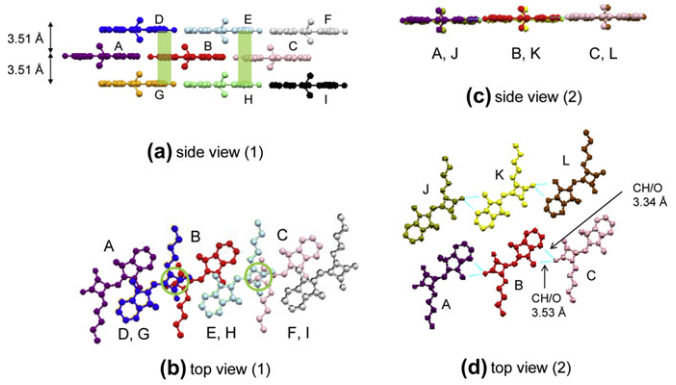

Fig. 7. Single X-ray crystallography of **11**.

Fig. 8 indicates the single X-ray crystallography of **12**. Molecules are arranged as a 'herring-bone' fashion with forming a pair of dimers. CH/O interactions are observed between B and J with the tilt angle 102.6° as shown in side view (2). Side view (1) and top view (1) show that molecules A and B form a pair of head-to-tail dimer. π/π-interactions are observed between A and B with interplanar distance 3.72 Å as shown in side view (3). Molecule F is located on the same plane to B with CH/O interactions. Side view (3) and top view (2) indicate that π/π-interactions are also observed between B and C at the squarate moiety with interplanar distance 3.40 Å. The same interactions are observed among C, D, and G as shown in top view (3). Thus, dye **12** has consecutive π/π stacking as shown in side view (3).

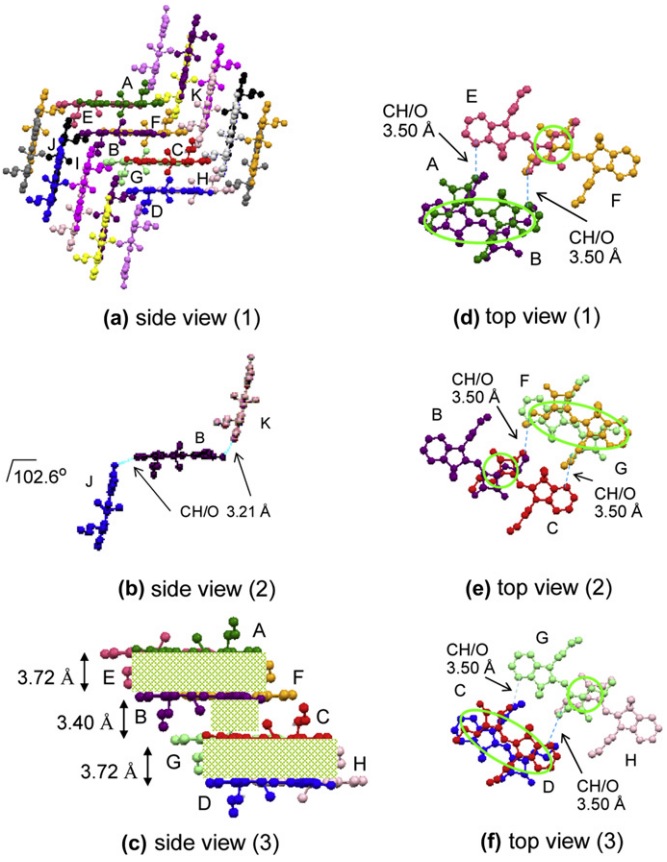

Fig. 8. Single X-ray crystallography of **12**.

The single X-ray crystallography of **13** is depicted in Fig. 9. A pair of dimers is arranged in a 'sandwich' fashion as shown in overview and side view (1). Side view (1) also indicates that the tilt angle between the dimers is 67.4°. No intermolecular interactions are observed between B and I. Side view (2) depicts that molecules A and B form a pair of head-to-tail dimers with two CH/π interactions. No π/π interactions are observed between A and B as shown in top view (2). Top view (1) and side view (3) depict that molecules A, C, D, and E are located almost on the same plain with CH/O interactions. Molecules F, G, B, and H are also arranged in parallel for C, D, A, and E with interplanar distance 3.27 Å π/π interactions are observed between the carbonyl groups of A and G. The same interactions are observed between B and E. Thus, dye **13** has isolated dimer-type packing.

Fig. 10 shows the single X-ray crystallography of **14**. Side view and top view (1) depict that molecules A, B, and C are located on the same plane and are aligned toward the same direction with CH/O interactions. Molecules B and E form a pair of head-to-tail dimer.

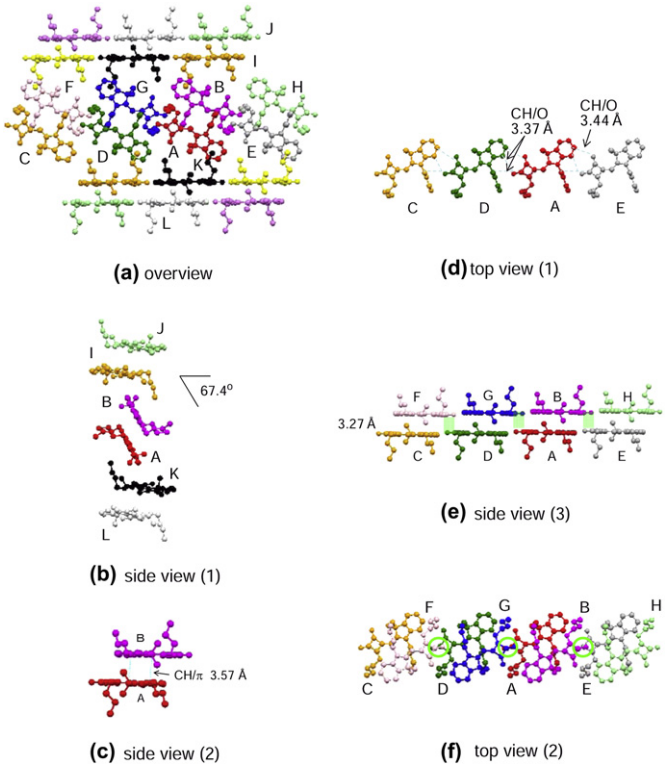

Fig. 9. Single X-ray crystallography of **13**.

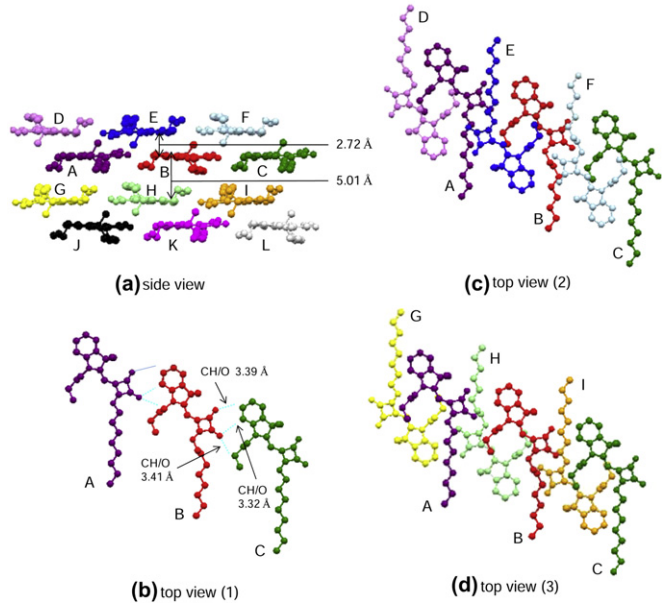

Fig. 10. Single X-ray crystallography of **14**.

Side view indicates that molecules D, E, and F are arranged in parallel for A, B, and C. However, no π/π overlapping is observed between B and E as well as between B and F as depicted in top view (2). Molecules G, H, and I are also arranged in parallel for A, B, and C with interplanar distance 5.01 Å, being too long to have interactions. Thus, dye **14** has isolated dimer-type packing.

Fig. 11 depicts the single X-ray crystallography of **15**. Molecules A and B form a pair of head-to-tail dimer with π/π interactions, the interplanar distance being 3.55 Å as shown in side view (1) and top view (1). Though molecule C is arranged in parallel for A, no π/π

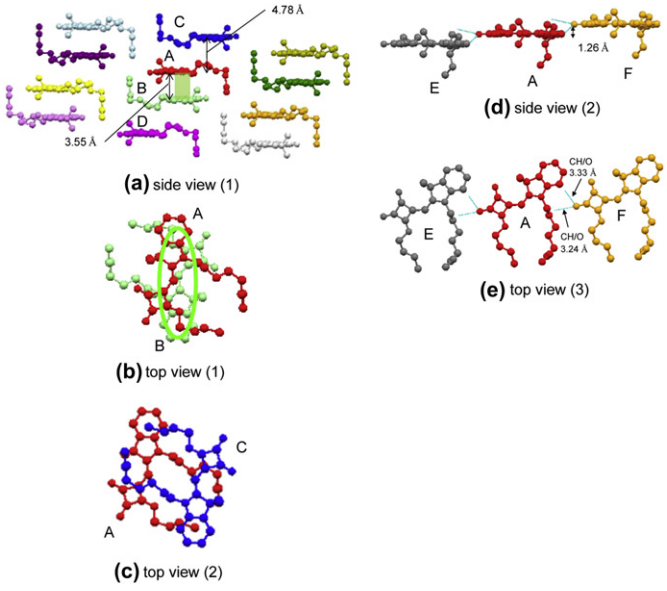

Fig. 11. Single X-ray crystallography of **15**.

overlapping is observed between them as shown in top view (2). Side view (2) and top view (3) indicate that molecules E and F are located almost on the same plane to A with CH/O interactions. Thus, dye **15** has isolated dimer-type packing.

The solid-state fluorescence intensity depends on the packing motif and melting point of the fluorophores. Consecutive π/π-interactions and hydrogen bonding can reduce the solid-state fluorescence intensity.[12] Furthermore, when the melting point is low, the internal conversion process comes from stretching, vibration, and rotation modes of the flexible linkages could be accelerated to decrease the solid-state fluorescence intensity.[13] As dyes **11** and **12** have consecutive π/π stacking, it is reasonable that their solid-state fluorescence intensity is low. Dyes **13**, **14**, and **15** have isolated dimer-type packing. No emission from the eximers was observed for **13**, **14**, and **15**. From only the view point of packing motif, dyes **13**, **14**, and **15** could show solid-state fluorescence. However, as the melting point of **14** (76.7 °C) and **15** (91.1) is significantly low compared with that of **13** (126.0), dye **13** could show strong solid-state fluorescence intensity. The intermolecular interactions of **13** in the aggregated form are supposed to be similar to those in the crystalline form. Therefore, semi-SQ dye **13** could show AIEE due to the free rotation inhibition of flexible C–O bonds in the aggregated form.

3. Conclusions

We have serendipitously found that 3-butoxy-4-(1-butyl-3,3-dimethyl-3*H*-indol-2-ylidenemethyl)-3-cyclobut-1,2-dione exhibited intense solid-state fluorescence (Φ_f=0.21) at F_{max} 536 and 563 nm in the crystalline form, whereas the other any derivatives showed very weak (Φ_f<0.02) or no fluorescence. This result is attributed to the isolated dimer-type packing and suitable melting point. This compound showed AIEE due to this packing motif and prevention of flexible C–O bond free rotation in the aggregated form.

4. Experimental

4.1. General

Melting points were measured with a Yanagimoto MP-S2 micro-melting-point apparatus. Those of **11**–**15** were measured by SII

Technology Co., EXSTAR-6000 instrument. NMR spectra were obtained by a JEOL ECX 400P spectrometer. MS spectra were measured with a JEOL MStation 700 spectrometer. UV–vis absorption, reflection, and fluorescence spectra were taken on Hitachi U-3500, U-4000, and F-4500 spectrophotometers, respectively. Fluorescence quantum yields were measured by a Hamamatsu Photonics Absolute PL Quantum Yield Measurement System C9920-02. 2,3,3-Trimethylindolenine (**1**), 1-butyl iodide (**3**), 1-octyl iodide (**4**), 3,4-dibutoxy-3-cyclobutene-1,2-dione (**9**), and 3,4-dihydroxy-3-cyclobutene-1,2-dione were purchased from Tokyo Kasei Co., Ltd. Methyl iodide (**2**) was purchased from Nacalai Tesque Co., Ltd. 2,3,3-Trimethyl-3*H*-indolium iodides **5**–**7** were synthesized as described in our previous paper.[8] 3,4-Dialkoxy-3-cyclobutene-1,2-diones **8** and **10** were prepared by the reaction of 3,4-dihydroxy-3-cyclobutene-1,2-dione with an alcohol followed by purification by column chromatography (SiO_2, CH_2Cl_2/AcOEt=20:1).

4.2. Synthesis of 3-alkoxy-4-(3,3-trimethyl-3*H*-indol-2-ylidenemethyl)-3-cyclobut-1,2-diones 11–15

An alcohol solution (**11**, **13**, **15**: BuOH; **12**, **14**: EtOH, 12 mL) of a 2,3,3-trimethyl-3*H*-indolium iodide **5**–**7** (8 mmol), a 3,4-dialkoxycyclobut-3-ene-1,2-dione **8**–**10** (8 mmol), and triethylamine (1.6 mL) was heated at 75 °C (**11**: 0.3 h; **12**, **14**: 2 h; **13**, **15**: 1 h). After the reaction was completed, to the mixture were added water (20 mL) and dichloromethane (50 mL). The dichloromethane layer was separated, washed with water (50 mL×3), and dried over anhydrous sodium sulfate. The solvent was removed in vacuo. The product was purified by silica gel column chromatography (CH_2Cl_2 then CH_2Cl_2/AcOEt=20:1) and recrystallized from hexane.

*4.2.1. 3-Butoxy-4-(1,3,3-trimethyl-3H-indol-2-ylidenemethyl)-3-cyclobut-1,2-dione (**11**).* Yield 1.6 g (60%); mp 125.3 °C (lit.[8] 126–128 °C); IR (KBr) ν 1769 cm^{-1}; ^1H NMR ($CDCl_3$) δ=1.00 (t, *J*=7.1 Hz, 3H), 1.51 (sex, *J*=7.1 Hz, 2H), 1.63 (s, 6H), 1.87 (quin, *J*=7.1 Hz, 2H), 3.37 (s, 3H), 4.86 (t, *J*=7.1 Hz, 2H), 5.37 (s, 1H), 6.90 (d, *J*=7.5 Hz, 1H), 7.07 (t, *J*=7.5 Hz, 1H), 7.26 (d, *J*=7.5 Hz, 1H), 7.28 (t, *J*=7.5 Hz, 1H); ^{13}C NMR ($CDCl_3$) δ=13.8, 18.8, 27.0 (2C), 30.0, 32.2, 47.9, 73.9, 81.6, 108.2, 122.0, 122.8, 127.9, 140.9, 143.2, 169.1, 173.6, 187.9, 187.9, 192.7; EIMS (70 eV) *m*/*z* (rel intensity) 325 (M^+, 72), 212 (100). Anal. Found: C, 74.01, H, 7.24; N, 4.19%. Calcd for $C_{20}H_{23}NO_3$: C, 73.82, H, 7.12; N, 4.30%.

*4.2.2. 4-(1-Butyl-3,3-dimethyl-3H-indol-2-ylidenemethyl)-3-ethoxy-3-cyclobut-1,2-dione (**12**).* Yield 1.0 g (37%); mp 120.6 °C; IR (KBr): ν 1769 cm^{-1}; ^1H NMR ($CDCl_3$) δ=1.00 (t, *J*=7.5 Hz, 3H), 1.45 (sex, *J*=7.5 Hz, 2H), 1.54 (t, *J*=7.1 Hz, 3H), 1.62 (s, 6H), 1.74 (quin, *J*=7.5 Hz, 2H), 3.82 (t, *J*=7.5 Hz, 2H), 4.90 (q, *J*=7.1 Hz, 2H), 5.41 (s, 1H), 6.88 (d, *J*=7.8 Hz, 1H), 7.07 (t, *J*=7.8 Hz, 1H), 7.27 (t, *J*=7.8 Hz, 1H), 7.27 (d, *J*=7.8 Hz, 1H); ^{13}C NMR ($CDCl_3$) δ=13.9, 16.0, 20.4, 27.0 (2C), 28.6, 42.9, 48.0, 70.0, 81.4, 108.5, 122.1, 122.7, 122.8, 141.0, 142.8, 168.5, 173.8, 187.5, 187.5, 192.6; FABMS (NBA) *m*/*z* 340 (MH^+). Anal. Found: C, 74.73, H, 7.61; N, 4.19. Calcd for $C_{21}H_{25}NO_3$: C, 74.31, H, 7.42; N, 4.13.

*4.2.3. 3-Butoxy-4-(1-butyl-3,3-dimethyl-3H-indol-2-ylidenemethyl)-3-cyclobut-1,2-dione (**13**).* Yield 1.6 g (56%); mp 126.0 °C (lit.[14] 128–129 °C); IR (KBr): ν 1772 cm^{-1}; ^1H NMR ($CDCl_3$) δ=1.00 (t, *J*=7.6 Hz, 3H), 1.01 (t, *J*=7.2 Hz, 3H), 1.45 (sex, *J*=7.6 Hz, 2H), 1.52 (sex, *J*=7.2 Hz, 2H), 1.62 (s, 6H), 1.74 (quin, *J*=7.6 Hz, 2H), 1.87 (quin, *J*=7.2 Hz, 2H) 3.82 (t, *J*=7.6 Hz, 2H), 4.86 (t, *J*=7.2 Hz, 2H), 5.42 (s, 1H), 6.89 (d, *J*=7.3 Hz, 1H), 7.07 (t, *J*=7.3 Hz, 1H), 7.27 (t, *J*=7.3 Hz, 1H), 7.28 (d, *J*=7.3 Hz, 1H); ^{13}C NMR ($CDCl_3$) δ=13.8, 13.9, 18.8, 20.4, 27.0 (2C), 28.6, 32.2, 42.8, 48.0, 73.8, 81.3, 108.5, 122.1, 122.7, 127.8, 141.0, 142.8, 168.4, 173.6, 187.6, 187.6, 192.8; EIMS (70 eV) *m*/*z* (rel intensity) 367 (M^+, 98), 254 (100), 242 (54), 226 (48) 212 (64), 149 (32). Anal. Found: C, 75.36, H, 8.00; N, 3.85. Calcd for $C_{23}H_{29}NO_3$: C, 75.17, H, 7.95; N, 3.81.

*4.2.4. 4-(1-Butyl-3,3-dimethyl-3H-indol-2-ylidenemethyl)-3-octyloxy-3-cyclobut-1,2-dione (**14**).* Yield 0.17 g (5%); mp 76.7 °C; IR (KBr): ν 1769 cm^{-1}; ^1H NMR ($CDCl_3$) δ=0.89 (t, *J*=7.1 Hz, 3H), 1.00 (t, *J*=7.6 Hz, 3H), 1.23–1.41 (m, 10H), 1.46 (quin, *J*=7.1 Hz, 2H), 1.62 (s, 6H), 1.74 (quin, *J*=7.6 Hz, 2H), 1.87 (quin, *J*=7.1 Hz, 2H), 3.82 (t, *J*=7.6 Hz, 2H), 4.85 (t, *J*=7.1 Hz, 2H), 5.42 (s, 1H), 6.88 (d, *J*=7.4 Hz, 1H), 7.07 (t, *J*=7.4 Hz, 1H), 7.27 (t, *J*=7.4 Hz, 1H), 7.28 (d, *J*=7.4 Hz, 1H); ^{13}C NMR ($CDCl_3$) δ=13.9, 14.2, 20.4, 22.7, 25.5, 27.0 (2C), 27.8, 28.6, 29.2, 30.2, 31.8, 42.8, 48.0, 74.1, 81.3, 108.5, 122.1, 122.7, 127.8, 141.0, 142.8, 168.4, 173.6, 187.6, 187.7, 192.8; EIMS (70 eV) *m*/*z* (rel intensity) 423 (M^+, 79), 254 (100). Anal. Found: C, 76.22, H, 8.95; N, 3.34. Calcd for $C_{27}H_{37}NO_3$: C, 76.56, H, 8.80; N, 3.31.

*4.2.5. 3-Butoxy-4-(1-octyl-3,3-dimethyl-3H-indol-2-ylidenemethyl)-3-cyclobut-1,2-dione (**15**).* Yield 1.3 g (39%); mp 91.1 °C; IR (KBr): ν 1769 cm^{-1}; ^{13}H NMR ($CDCl_3$) δ=0.88 (t, *J*=7.5 Hz, 3H), 1.01 (t, *J*=7.3 Hz, 3H), 1.20–1.45 (m, 10H), 1.51 (sex, *J*=7.3 Hz, 2H), 1.62 (s, 6H), 1.74 (quin, *J*=7.5 Hz, 2H), 1.86 (quin, *J*=7.3 Hz, 2H), 3.81 (t, *J*=7.5 Hz, 2H), 4.86 (t, *J*=7.3 Hz, 2H), 5.41 (s, 1H), 6.87 (d, *J*=7.8 Hz, 1H), 7.07 (t, *J*=7.8 Hz, 1H), 7.27 (t, *J*=7.8 Hz, 1H), 7.28 (d, *J*=7.8 Hz, 1H); ^{13}C NMR ($CDCl_3$) δ=13.8, 14.1, 18.8, 22.7, 26.4, 27.0 (2C), 27.1, 29.2, 29.3, 31.8, 32.2, 43.1, 48.0, 73.8, 81.3, 108.5, 122.1, 122.7, 127.8, 141.0, 142.8, 168.4, 173.6, 187.6 (2C), 192.8; EIMS (70 eV) *m*/*z* (rel intensity) 423 (M^+, 91), 330 (100), 212 (72). Anal. Found: C, 76.46, H, 8.86; N, 3.38. Calcd for $C_{27}H_{37}NO_3$: C, 76.56, H, 8.80; N, 3.31.

4.3. Synthesis of 4-(1-butyl-3,3-dimethyl-3*H*-indol-2-ylidenemethyl)-3-hydroxy-3-cyclobut-1,2-dione (16)

To 40% aqueous sodium hydroxide (0.12 mL, 0.85 mmol) was added an ethanol solution (4 mL) of **13** (0.367 g, 1 mmol). The mixture was refluxed for 5 min. After the reaction was completed, to the mixture was added 2 N hydrochloric acid (1.2 mL). Then, the solvent was evaporated in vacuo. The product was purified by silica gel column chromatography (CH_2Cl_2/MeOH=10:1). Yield 0.087 g (28%); mp 102–103 °C (lit.[8] 102–103 °C); IR (KBr): ν 3443, 1763 cm^{-1}; ^1H NMR ($CDCl_3$) δ=0.97 (t, *J*=7.4 Hz, 3H), 1.44 (sex, *J*=7.4 Hz, 2H), 1.61 (s, 6H), 1.70 (quin, *J*=7.4 Hz, 2H), 3.84 (t, *J*=7.4 Hz, 2H), 5.70 (s, 1H), 6.93 (d, *J*=7.8 Hz, 1H), 6.96 (t, *J*=7.8 Hz, 1H), 7.21 (t, *J*=7.8 Hz, 1H), 7.25 (d, *J*=7.8 Hz, 1H); ^{13}C NMR ($CDCl_3$) δ=13.6, 22.0, 26.8 (2C), 28.3, 41.9, 46.1, 82.7, 107.3, 120.9, 121.4, 127.3, 140.6, 143.5, 163.6, 180.3 (2C), 196.2, 203.1; FABMS (NBA) *m*/*z* 312 (MH^+). Anal. Found: C, 73.45, H, 6.58; N, 4.30. Calcd for $C_{19}H_{21}NO_3$: C, 73.29, H, 6.80; N, 4.50.

4.4. Single X-ray crystallographic analysis

Single crystals were obtained by diffusion method using dichloromethane and hexane. The diffraction data were collected by using graphite monochromated Mo-K_α radiation (λ=0.71069 Å). The structure was solved by direct methods SIR97 and refined by fill-matrix least-squares calculations.

Crystal data for **11**: $C_{20}H_{23}NO_3$, M_w=325.39, monoclinic, *C*2/m, *Z*=4, *a*=23.826(16), *b*=7.023(5), *c*=11.065(8) Å, α=90, β=112.071(8), γ=90°, D_{calcd}=1.260 g cm^{-3}, *T*=123(2) K, *F*(000)=696, μ=0.084 mm^{-1}, 6875 reflections were corrected, 2094 unique (R_{int}=0.0327). 2094 observed ($I>2\sigma(I)$), 162 parameters, R_1=0.0623, wR_2=0.1229.

Crystal data for **12**: $C_{21}H_{25}NO_3$, *Mw*=339.42, monoclinic, *P*21/n, *Z*=4, *a*=9.389(4), *b*=20.255(8), *c*=10.201(4) Å, α=90, β=105.020(6), γ=90°, D_{calcd}=1.203 g cm^{-3}, *T*=123(2) K, *F*(000)=728, μ=0.080 mm^{-1}, 15,160 reflections were corrected, 4285 unique

(R_{int}=0.0375). 4285 observed ($I>2\sigma$ (I)), 298 parameters, R_1=0.0667, wR_2=0.1162.

Crystal data for **13**: $C_{23}H_{29}NO_3$, Mw=367.47, monoclinic, $P2_1/n$, Z=4, a=10.849(4), b=10.654(4), c=19.083(7) Å, α=90, β=106.919(4), γ=90°, D_{calcd}=1.157 g cm^{-3}, T=123(2) K, F(000)=792, μ=0.076 mm^{-1}, 16,641 reflections were corrected, 4817 unique (R_{int}=0.0358). 4817 observed ($I>2\sigma$ (I)), 317 parameters, R_1=0.0663, wR_2=0.1342.

Crystal data for **14**: $C_{27}H_{37}NO_3$, Mw=423.58, triclinic, P-1, Z=4, a=13.011(4), b=13.775(4), c=14.943(5) Å, α=74.868(10), β=88.342(13), γ=69.521(10)°, D_{calcd}=1.164 g cm^{-3}, T=123(2) K, F(000)=920, μ=0.075 mm^{-1}, 19,866 reflections were corrected, 10,963 unique (R_{int}=0.0438). 10,963 observed ($I>2\sigma$ (I)), 855 parameters, R_1=0.0767, wR_2=0.1420.

Crystal data for **15**: $C_{27}H_{37}NO_3$, Mw=423.58, triclinic, P-1, Z=4, a=9.093(3), b=10.930(4), c=25.485(10) Å, α=89.034(12), β=84.089(11), γ=72.177(9)°, D_{calcd}=1.173 g cm^{-3}, T=123(2) K, F(000)=920, μ=0.075 mm^{-1}, 19,595 reflections were corrected, 10,829 unique (R_{int}=0.0359). 10,829 observed ($I>2\sigma$ (I)), 775 parameters, R_1=0.0812, wR_2=0.1570.

Crystallographic data (**11** (CCDC 696948), **12** (CCDC 696951), **13** (CCDC 696949), **14** (CCDC 696952), and **15** (CCDC 696950)) have been deposited at the CCDC, 12 Union Road, Cambridge CB2 1EZ, UK.

Supplementary data

These data include ^{1}H NMR spectra of **11**, **12**, **13**, **14**, **15**, and **16**, UV–vis absorption and fluorescence spectra of **13** in various solvents, and single X-ray crystallographic data for **11**, **12**, **13**, **14**, and **15**. Supplementary data related to this article can be found at http://dx.doi.org/10.1016/j.tet.2012.09.089.

References and notes

1. (a) Lee, M.-T.; Yen, C.-K.; Yang, W.-P.; Chen, H.-H.; Liao, C.-H.; Tsai, C.-H. *Org. Lett.* **2004**, *6*, 1241; (b) Swanson, S. A.; Wallraff, G. M.; Chen, J. P.; Zhang, W.; Bozano, L. D.; Carter, K. R.; Salem, J. R.; Villa, R.; Scott, J. C. *Chem. Mater.* **2003**, *15*, 2305; (c) Chen, C.-T.; Chiang, C.-L.; Lin, Y.-C.; Chan, L.-H.; Huang, C.-H.; Tsai, Z.-W.; Chen, C.-T. *Org. Lett.* **2003**, *5*, 1261.
2. (a) Zhang, D.; Zhang, S.; Ma, D.; Gulimina; Li, X. *Appl. Phys. Lett.* **2006**, *89*, 231112; (b) Jones, G., II; Rahman, M. A. *J. Phys. Chem.* **1994**, *98*, 13028.
3. (a) Wang, X.; Morales, A. R.; Urakami, T.; Zhang, L.; Bondar, M. V.; Komatsu, M.; Belfield, K. D. *Bioconjugate Chem.* **2011**, *22*, 1438; (b) Xu, J.-P.; Fang, Y.; Song, Z.-G.; Mei, J.; Jia, L.; Qin, A. J.; Sun, J. Z.; Ji, J.; Tang, B. Z. *Analyst* **2011**, *136*, 2315; (c) Song, P.; Chen, X.; Xiang, Y.; Huang, L.; Zhou, Z.; Wei, R.; Tong, A. *J. Mater. Chem.* **2011**, *21*, 13470; (d) Shundo, A.; Okada, Y.; Ito, F.; Tanaka, K. *Macromolecules* **2012**, *45*, 329; (e) Fujishima, S.-H.; Nonaka, H.; Uchinomiya, S.-H.; Kawase, Y. A.; Ojida, A.; Hamachi, I. *Chem. Commun.* **2012**, 594.
4. For example Law, K.-Y.; Bailey, F. C. *J. Org. Chem* **1992**, *57*, 3278.
5. Nakazumi, H.; Natsukawa, K.; Nakai, K.; Isagawa, K. *Angew. Chem., Int. Ed. Engl.* **1994**, *33*, 1001.
6. (a) Yagi, S.; Nakai, K.; Hyodo, Y.; Nakazumi, H. *Synthesis* **2002**, 413; (b) Yagi, S.; Fujie, Y.; Hyodo, Y.; Nakazumi, H. *Dyes Pigm.* **2002**, *52*, 245.
7. (a) Avirah, R. R.; Jyothish, K.; Ramaiah, D. *Org. Lett.* **2007**, *9*, 121; (b) Bae, J. S.; Gwon, S. Y.; Son, Y. A.; Kim, S. H. *Dyes Pigm.* **2009**, *83*, 324.
8. Matsui, M.; Mase, H.; Jin, J.; Funabiki, K.; Yoshida, T.; Minoura, H. *Dyes Pigm.* **2006**, *70*, 48.
9. (a) Hong, Y.; Lam, J. W. Y.; Tang, B. Z. *Chem. Commun.* **2009**, 4332 and references cited therein; (b) Yuan, W. Z.; Lu, P.; Chen, S.; Lam, J. W. Y.; Wang, Z.; Liu, Y.; Kwok, H. S.; Ma, Y.; Tang, B. Z. *Adv. Mater. (Weinheim, Ger.)* **2010**, *22*, 2159; (c) Luo, J.; Xie, Z.; Lam, J. W. Y.; Cheng, L.; Chen, H.; Qiu, C.; Kwok, H. S.; Zhan, X.; Liu, Y.; Zhu, D.; Tang, B. Z. *Chem. Commun.* **2001**, 1740.
10. Zhao, Z.; Chen, S.; Lam, J. W. Y.; Jim, C. K. W.; Chan, C. Y. K.; Wang, Z.; Lu, P.; Deng, C.; Kwok, H. S.; Ma, Y.; Tang, B. Z. *J. Phys. Chem. C* **2010**, *114*, 7963.
11. (a) Itami, K.; Ohashi, Y.; Yoshida, J. *J. Org. Chem* **2005**, *70*, 2778; (b) Ning, Z.; Chen, Z.; Zhang, Q.; Yan, Y.; Qian, S.; Cao, Y.; Tian, H. *Adv. Funct. Mater.* **2007**, *17*, 3799.
12. For example, (a) Shimizu, M.; Asai, Y.; Takeda, Y.; Yamatani, A.; Hiyama, T. *Tetrahedron Lett.* **2011**, *52*, 4084; (b) Imoto, M.; Ikeda, H.; Ohashi, M.; Takeda, M.; Tamaki, A.; Taniguchi, H.; Mizuno, K. *Tetrahedron Lett.* **2010**, *51*, 5877; (c) Zhao, C.-H.; Zhao, Y.-H.; Pan, H.; Fu, G.-L. *Chem. Commun.* **2011**, 5518; (d) Matsui, M.; Ikeda, R.; Kubota, Y.; Funabiki, K. *Tetrahedron Lett.* **2009**, *50*, 5047; (e) Ooyama, Y.; Nabeshima, S.; Mamura, T.; Ooyama, H. E.; Yoshida, K. *Tetrahedron* **2010**, *66*, 7954.
13. An, P.; Shi, Z.-F.; Dou, W.; Cao, X.-P.; Zhang, H. L. *Org. Lett.* **2010**, *12*, 4364.